Design of Low Actuation Voltage RF MEMS Switch

Sergio P. Pacheco[1], Linda P. B. Katehi[1], and Clark T.-C. Nguyen[2]

[1]Radiation Laboratory and [2]Center for Microsystems
Department of Electrical Engineering and Computer Science
University of Michigan
Ann Arbor, Michigan 48109-2122 USA

ABSTRACT

Low-loss microwave microelectromechanical systems (MEMS) shunt switches are reported that utilize highly compliant serpentine spring folded suspensions together with large area capacitive actuators to achieve low actuation voltages while maintaining sufficient off-state isolation. The RF MEMS switches were fabricated via a surface micromachining process using PI2545 Polyimide [1] as the sacrificial layer. The switch structure was composed of electroplated nickel and the serpentine folded suspensions had varying number of meanders from 1 to 5. DC measurements indicate actuation voltages as low as 9 V with an on-to-off capacitance ratio of 48. Power handling measurement results showed no "self-biasing" or failure of the MEMS switches for power levels up to 6.6W. RF measurements demonstrate an isolation of -26 dB at 40 GHz.

I. INTRODUCTION

The advent of bulk and surface micromachining techniques during the 1970s enabled the emergence of microelectromechanical systems (MEMS). Micromechanical microwave switches were first demonstrated by Petersen as cantilever beams using electrostatic actuation [1]. The advantage of MEMS switches over their solid state counterparts such as FETs or PIN diodes is their extremely low series resistance and low drive power requirements. In addition, since MEMS switches do not contain a semiconductor junction, they exhibit negligible intermodulation distortion.

Recently, shunt microwave switches have been developed in the K/Ka band [2], [3], [4]. These devices are primarily designed for low-loss applications that do not require fast rates such as airborne and/or deep space communication. The switches are usually electrostatic in nature and commonly driven by bias voltages in the 30 - 50 V range. The primary goal of the research presented in this paper is to develop electrostatic shunt K/Ka-band microwave switches that rival the performance of the above designs while achieving very low pull-in voltages. This is achieved by designing switch structures with extremely compliant folded suspension springs and large electrostatic actuation area.

[1]DuPont Electronic Materials, P. O. Box 80334, Wilmington, DE.

II. MECHANICAL AND RF DESIGN

Figure 1 shows a Scanning Electron Micrograph (SEM) of a released MEMS RF switch with serpentine folded suspensions containing four meanders.

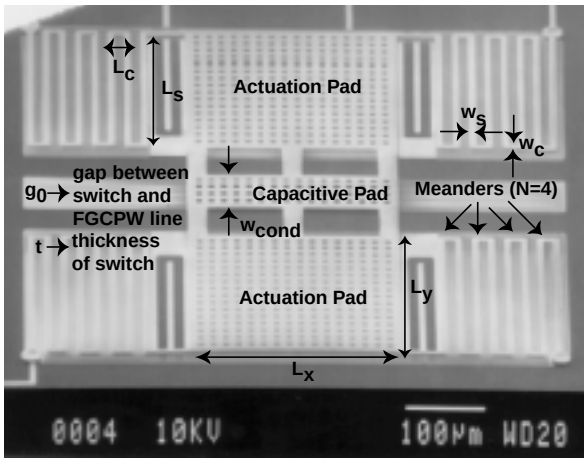

Fig. 1. SEM of fabricated MEMS RF switch.

TABLE I
PHYSICAL DIMENSIONS OF MEMS MICROWAVE SWITCH SHOWN IN FIG. 1

L_s	250μm	L_x	250μm
L_c	20μm	L_y	250μm
t	2μm	w_{cond}	60μm
w	5μm	g_0	3μm
N	4	K_z	0.521 N/m
mass	3.23x10^{-9}kg	V_{pi}	1.94 V

Table I lists the physical dimensions of the MEMS microwave switch shown in Fig. 1.

The mechanical design consists of folded suspensions of serpentine format attached to square plates that provide the electrostatic area of actuation. Attached to the actuation plates is the center plate that provides the parallel capacitance at the center conductor of the finite ground coplanar waveguide (FGCPW) line. The entire structure is anchored

0-7803-5687-X/00/$10.00 (c) 2000 IEEE

to the substrate at the ends of the folded suspensions. At the moment of actuation, the necessary pull-in voltage is applied between the ground plane of the FGCPW line and the switch. Once the switch clamps down, the high capacitance present at the center conductor provides a virtual short at RF.

The formula for actuation or pull-in voltage is given by:

$$V_{pi} = \sqrt{\frac{8K_z g_o^3}{27A\epsilon_o}} \tag{1}$$

where K_z is the spring constant in the z-direction, g_o is the initial gap between the switch and the bottom electrode, A is the area of the actuation pads and ϵ_o is the permittivity of air. In order to lower the pull-in voltage of the structure, three different routes can be pursued: (1) increasing the area of actuation, (2) diminishing the gap between the switch and bottom electrode, and (3) designing a structure with low spring constant. In the first case, the area can only be increased by so much before compactness becomes a prevailing issue. In the second case, the return loss associated with the RF signal restricts the value of the gap. The third route is the one with the most flexibility, since the design of the springs does not considerably impact the size, weight, and/or RF performance of the circuit.

The design of the folded suspension is of crucial importance in realizing MEMS switches with low actuation voltage. The folded suspension was chosen due to its ability to provide very low values of spring constant in a compact area as well as providing high cross-axis sensitivity between vertical and lateral dimensions. The spring constant in the z-direction, k_z for one of the suspensions is given by [5], [6]:

$$k_z = \frac{Ew\left(\frac{t}{L_c}\right)^3}{1+\frac{L_s}{L_c}\left(\left(\frac{L_s}{L_c}\right)^2+12\frac{1+\nu}{1+\left(\frac{w}{t}\right)^2}\right)} \tag{2}$$

where E and ν are the Young's modulus and Poisson's ratio for the metal. The total spring constant is the sum of all four suspensions attached to the structure:

$$K_z = \frac{4k_z}{N} \tag{3}$$

where N is the number of meanders in the suspension (Figure 1 contains four meanders). The spring constant decreases linearly with successive addition of meanders to the folded suspension.

Five MEMS switch designs were fabricated and measured. All designs were identical except for containing different number of meanders in their folded suspensions. MEMS switches with one, two, three, four and five meanders were studied.

III. Fabrication Process

A five mask batch process is used to fabricate the MEMS switching circuits. The samples are composed of 400 μm high-resistivity silicon. Figure 2 shows the process flow used to fabricate the MEMS RF switches.

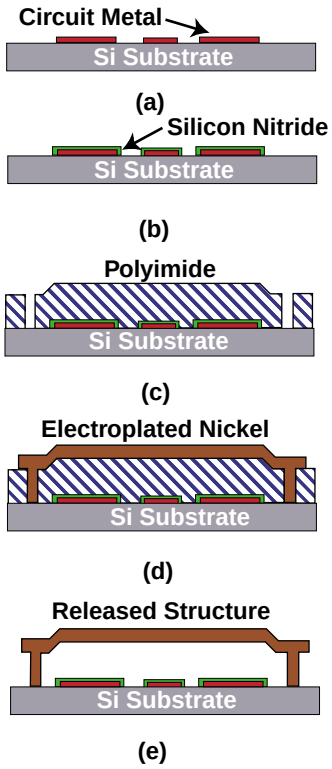

Fig. 2. Process flow for MEMS RF switch.

The process is as follows: (a) 500/7500Å of Ti/Au is deposited and the circuit metal layer is defined via a liftoff process; (b) 1000Å of plasma enhanced chemical vapor deposition (PECVD) silicon nitride (Si_3N_4) is patterned over the locations of switch actuation; (c) a sacrificial layer 3μm thick of polyimide DuPont PI2545 is spun cast, soft baked, and patterned for anchor points; (d) 2μm of nickel is electroplated to define the switch structure; (e) sacrificial etching of the polyimide layer and supercritical CO_2 drying and release of the switch structure.

IV. Results and Discussion

Actuation voltage measurements were performed using a HP 4275A Multi-Frequency LCR meter with an internal bias option.

Table II lists the predicted and measured values for pull-in voltages for each given suspension design. As expected, the actuation voltage dropped with increasing number of meanders. However, the values are considerably higher than the calculated design values. This increase can be tracked to several factors. First, a slight overplating of the beam struc-

TABLE II
MEASURED ACTUATION VOLTAGES FOR MEMS SWITCH

Number of meanders	V_{pi} - Design	V_{pi} - Measured
1	3.90 V	35 V
2	2.75 V	28 V
3	2.24 V	20 V
4	1.94 V	15 V
5	1.74 V	9 V

ture to 2.6μm instead of the design value of 2μm accounts for an increase of 1.48 times in the actuation voltage. Second, the structures exhibit a certain amount of warping in the folded suspensions due to vertical stress gradients across the thickness of the beams. This causes the actuation pads to be approximately 5μm above the ground planes upon release, thus increasing the pull-in voltage by an additional factor of 2.15. Third, the remaining increase is due to the high intrinsic residual axial tensile stress developed in the nickel film during the fabrication process (in the order of 150 MPa).

Figure 3 shows the actuation of the circuits and the respective on and off capacitances. The on and off capacitances

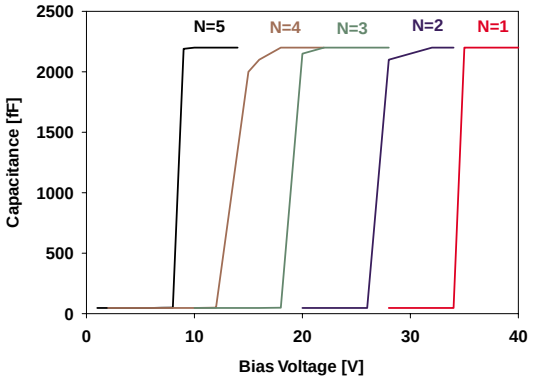

Fig. 3. Plot of measured pull-in voltage vs. capacitance for varying number of spring meanders.

were measured at 47 fF and 2.25 pF respectively, resulting in an on-to-off ratio of 48.

The power handling capabilities of the RF MEMS were measured at X-Band. Fig. 4 is a diagram of the power measurement setup. The power source was an X-band (8-12 GHz) TWT amplifier and the variable attenuator was used to vary the output power from 1 mW up to the maximum level of 6.6 W. The power coming out of the MEMS switch was coupled to a 20 dB attenuator and fed into the power meter.

The power handling capabilities of the RF MEMS switches can be limited either by the current density on the

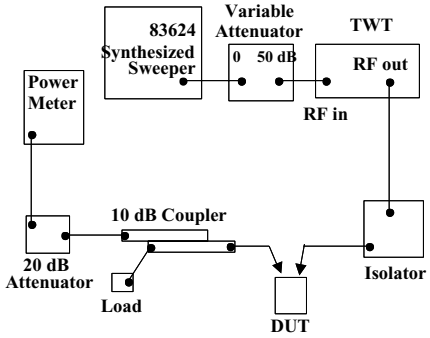

Fig. 4. X-band power measurement set-up

transmission line causing excessive heating or by the actuation of the switches due to the average RF voltage on the FGCPW line (denoted as "self biasing"). Since the electrostatic force acting on the switch can derive from either a positive or negative voltage, the average voltage level of the rectified sine wave due to the RF power on the FGCPW line is attracting the switch.

The predicted average voltage on the FGCPW line for the maximum power level of 6.6 W is 8.56V, which is not enough to cause any of the switch designs to actuate. Actually, since the RF power is delivered to the center conductor of the FGCPW line, the area of electrostatic attraction is approximately eight times smaller and a pull-in voltage of 26 V would be needed to actuate a MEMS switch with five meanders. That pull-in voltage corresponds to a RF power level of 66.6 W. As predicted, the MEMS switch did not "self-bias" at any moment. Fig. 5 shows a plot of the power readings for the cases of the switch off and on.

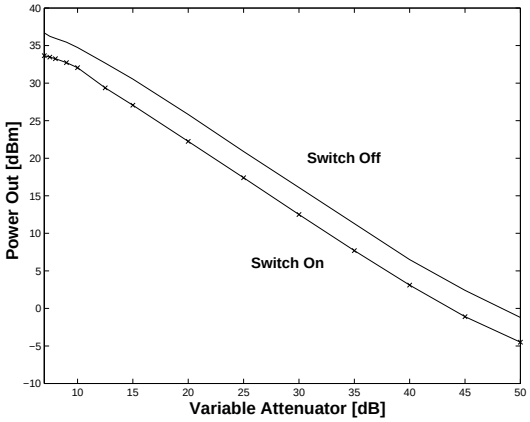

Fig. 5. Measured power levels for switch off (-) and switch on (x)

Switches were actuated using bias voltages from 10-40 V at power levels from 1mW to 5.5W. There was no observed catastrophic failure of the switches and/or dielectric film. The dielectric strength for a PECVD Si_3N_4 thin film is 5x10^6 V/cm [7], corresponding to a breakdown voltage of

50 V for a 1000Å thick film. There was a slight bending of the folded suspensions at power levels above 4.5 W with the switch on. The suspensions reverted back to their original position once the power was decreased or turned off. This warping was due to heating of the circuit as the power levels increased.

The RF response of the system was measured using a 8510C Vector Network Analyzer, Alessi Probe Station, and GGB Picoprobe 150 micron pitch coplanar probes. A TRL calibration software, MULTICAL, developed at NIST [8], [9] is used to deembed the effects of the probe tips and feedlines from the measurement response thus extending the reference plane up to the MEMS switch under test. The plot in Fig. 6 shows the response of the FGCPW line with a switch in the off position. Notice the increase of the return loss at

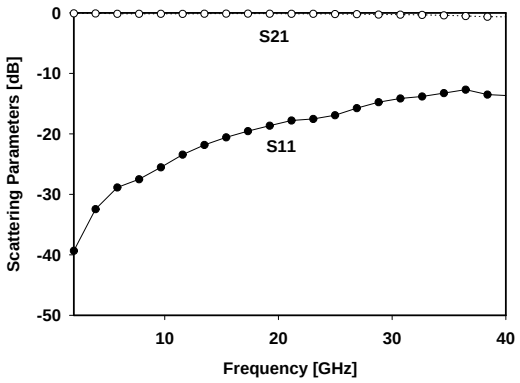

Fig. 6. Plot of measured RF response of FGCPW line with switch in off position.

higher frequencies due to the capacitance introduced by the switch. In addition, the difference in insertion loss as compared to a FGCPW line without a switch is was measured to be of only 0.16 dB at 40 GHz.

The RF characteristics with the switch on is shown in Fig. 7 and demonstrates an isolation of approximately -26 dB at 40 GHz. The isolation can be further improved by decreasing the thickness of the dielectric between the switch and center conductor, thus increasing the on capacitance. However, care must be taken in order to make sure that the thin film thickness is sufficient not to cause dielectric breakdown and current flow.

V. Conclusions

MEMS RF switches with actuation voltages as low as 9 V and excellent RF characteristics have been demonstrated. Measurements show an isolation of better than -15 dB above 15 GHz. These MEMS switches are suitable for wireless

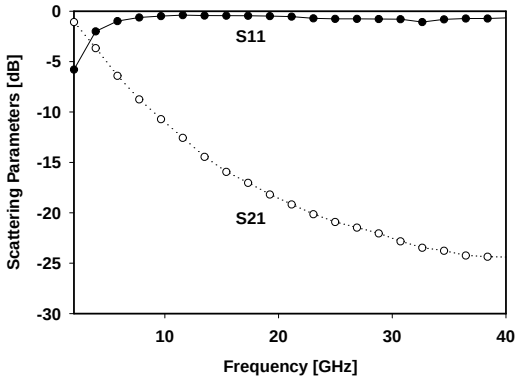

Fig. 7. Plot of measured RF response of FGCPW line with switch in off position.

and/or space systems where low power consumption is essential.

VI. Acknowledgments

The authors at the University of Michigan gratefully acknowledge the support of this research by the SOAC/JPL under the CISM Project and the Department of Defense Research and Engineering (DDR&E) Multidisciplinary University Research Initiative (MURI) on “Low Power Electronics” managed by the Army Research Office (ARO) under Grant DAAH04–96–1–0001.

References

[1] K. E. Petersen, “Micromechanical membrane switches on silicon,” *IBM Journal of Research and Development*, vol. 23, pp. 376–385, July 1971.

[2] C. Goldsmith, T. H. Lin, B. Powers, W. R. Wu, and B. Norvell, “Micromechanical membrane switches for microwave applications,” in *IEEE MTT-S International Microwave Symposium Proceedings*, pp. 91–94, 1995.

[3] J. J. Yao and M. F. Chang, “A surface micromachined miniature switch for telecommunications applications with signal frequencies from dc up to 4 GHz,” in *The 8th International Conference on Solid-State Sensors and Actuators Digest*, pp. 384–387, 1995.

[4] C. Goldsmith, J. Randall, S. Eshelman, and T. H. Lin, “Characteristics of micromachined switches at microwave frequencies,” in *IEEE MTT-S International Microwave Symposium Proceedings*, pp. 1141–1144, 1996.

[5] E. P. Popov, *Introduction to Mechanics of Solids*. Prentice-Hall, 1968.

[6] J. E. Shigley and L. D. Mitchell, *Mechanical Engineering Design*. McGraw-Hill, 4^{th} ed., 1983.

[7] M. Madou, *Fundamentals of Microfabrication*. New York: CRC Press, 1997.

[8] R. B. Marks and D. F. Williams, “Program multical,” tech. rep., NIST, August 1995. Rev. 1.

[9] R. B. Marks, “A multiline method of network analyzer calibration,” *IEEE Transactions on Microwave Theory and Techniques*, vol. 39, pp. 1205–1215, July 1991.